ISSN: 0976-3376

Available Online at http://www.journalajst.com

ASIAN JOURNAL OF SCIENCE AND TECHNOLOGY

Asian Journal of Science and Technology
Vol. 17, Issue, 06, pp. 14312-14321, June, 2026

RESEARCH ARTICLE

SYNTHESIS, MOLECULAR DOCKING, AND ANTIMICROBIAL EVALUATION OF PYRAZOLE-BASED SCHIFF-BASE DERIVATIVES USING A GREEN SOLVENT APPROACH

***[1]Purvi Joshi, [1]Paritri Upadhyay, [1]Yash Adodariya, [1]Vikram Vanol [2]Gaurav Sanghvi and [1]Dr. Shailesh Thakrar**

[1]Department of Chemistry, Christ College Rajkot - 360005, India
[2]Department of Microbiology, Marwadi University Rajkot - 360003, India

ARTICLE INFO

Article History:
Received 24th March, 2026
Received in revised form
16th April, 2026
Accepted 28th May, 2026
Published online 30th June, 2026

Key words:
Pyrazole, Schiff base, Green chemistry, Anti-microbial activities, 2-methyltetrahydrofuran, Molecular docking.

***Corresponding author:**
Dr. Shailesh Thakrar

ABSTRACT

The investigation of green chemistry approaches in medicinal chemistry has been prompted by the growing need for efficient and ecologically friendly chemical synthesis methods. These articles emphasize environmentally friendly pyrazole derivative synthesis techniques, which are good substitutes for synthetic techniques that uphold green principles. They also focus on Schiff bases, formed by condensing carbonyl compounds and primary amines, which have diverse industrial and biomedical applications, and their synthesis is being made more sustainable through green chemistry. In this study, we present the synthesis of (Z)-1,5-dimethyl-4-(((3-(3-nitrophenyl)-1-phenyl-1H-pyrazol-4-yl) methylene) amino)-2-phenyl-1,2-dihydro-3H-pyrazol-3-one(9a-9j). This was achieved through the condensation of 4-amino-1,5-dimethyl-2-phenyl-1,2-dihydro-3H-pyrazol-3-one with a 1,3-diphenyl-1H-pyrazole-4-carbaldehyde derivative, utilizing the green solvent 2-methyltetrahydrofuran. The characterization of all newly synthesized compounds was accomplished through spectral data analysis, including IR, 1H and 13C NMR spectroscopy, and mass spectrometry. The antimicrobial activity of the synthesized organic molecule derivatives was evaluated against a diverse array of microorganisms, including gram-positive and gram-negative bacteria and pathogenic fungi. To further investigate this, molecular docking studies were conducted to determine the binding affinity and interaction patterns of the synthesized compounds (9a-9j) with the crystal structure of the Staphylococcus aureus (3GR6) target protein.

Citation: ***Purvi Joshi, Paritri Upadhyay, Yash Adodariya, Vikram Vanol Gaurav Sanghvi and Shailesh Thakrar.*** **2026.** "Synthesis, Molecular Docking, and Antimicrobial Evaluation of Pyrazole-Based Schiff-base Derivatives using a Green Solvent Approach", *Asian Journal of Science and Technology*, 17, (06), 14312-14321.

INTRODUCTION

Among the various heterocyclic compounds, nitrogen-containing heterocycles have captured significant interest from researchers due to their versatile bioactive properties (1). Nitrogen is notably stable, exhibiting characteristics similar to inert gases, and does not readily react with other elements. Its availability and stability make it crucial in both the pharmaceutical and agricultural sectors (1, 2). Pyrazole, a prominent category of heterocyclic compounds, serves as a compelling framework in medicinal chemistry and is associated with several commercial medications, including Sildenafil, Zometapine, Celecoxib, and Rimonabant (3). The presence of two functionalities with differing reactivity within the pyrazole structure offers opportunities to introduce diversity into pyrazole frameworks, which may hold substantial medicinal significance. Numerous therapeutic agents, such as phenylbutazone, oxyphenbutazone, and Antipyrine, are classified as pyrazoles (4). Schiff bases, or imines, represent a significant class of compounds formed through the condensation of carbonyl compounds and primary amines. These molecules have been extensively investigated due to their wide-ranging industrial and biomedical applications (5). Their increasing significance is attributed to their diverse pharmacological properties, including antibacterial (6), antifungal, antimalarial (6), anti-inflammatory, and antiviral activities (5). Schiff bases have emerged as promising candidates for addressing drug resistance (7). A series of Schiff bases have been synthesized using pyrazole-containing amines and aldehydes (7). In alignment with our research on Schiff base compounds and their applications, the pyrazole nucleus was incorporated into the structure of the imine ligand to identify compounds that enhance bioactivity (5, 8). Pharmaceutical research has concentrated on developing novel therapeutic agents with heterocyclic cores (3). The extensive medical applications of pyrazoles,primarily focusing on their antibacterial, antifungal, anti-inflammatory, analgesic (9), and anxiolytic properties, have established them as an exceptional scaffold for the synthesis of physiologically active molecules (10). This study focuses on the synthesis of pyrazole-containing derivatives by employing a range of solvents to explore their effects on reaction efficiency and product yield. The selection of solvents was carefully considered to optimize the reaction environment, enhancing solubility, reactivity, and selectivity toward the target compounds. By systematically varying solvent conditions, the study aimed to identify the optimal

medium that facilitates the formation of pyrazole derivatives with high purity and yield (16, 17). All synthesized compounds subjected to antimicrobial evaluation against four bacterial strains (B. cereus and S. aureus, E. coli and P. aerugionosa) and two fungal stains (Candida albicans and Candida Tropicalis). The favourable biological activities of the synthesized compounds emphasize their promising application in the development of new antimicrobial and antifungal agents (14, 15). Molecular docking studies were conducted to further explore the binding affinity and interaction patterns of the synthesized compounds with the crystal structure of the Staphylococcus aureus (3GR6) target protein.

RESULT AND DISCUSSION

The synthesis of pyarazol based Schiff-base scaffolds was performed as outlined in Scheme 1. In an initial ethanol solution, a mixture comprising 1-methyl-2-phenylhydrazine (**1**) and ethyl 3-oxobutanoate (**2**) was catalyzed through the addition of 2-3 drops of acetic acid. The reaction mixture underwent reflux for a duration of 3–4 hours to promote both condensation and cyclization processes. Upon cooling to room temperature, a solid product was obtained. The crude product, 1,5-Dimethyl-2-phenyl-1,2-dihydro-3H-pyrazol-3-one (**3**), was collected by filtration and washed with cold ethanol to eliminate any impurities. Subsequently, this product was nitrated using concentrated nitric acid in glacial acetic acid, with the reaction conducted at 0–5 °C under stirring and then allowed to reach room temperature. Upon completion, the mixture was quenched in ice water, precipitating the product, which was then filtered, washed, and recrystallized. This process yields 1,5-dimethyl-4-nitro-2-phenyl-1,2-dihydro-3H-pyrazol-3-one (4) via electrophilic substitution at the 4-position. The compound 1,5-Dimethyl-4-nitro-2-phenyl-1,2-dihydro-3H-pyrazol-3-one (4) is subsequently reduced to 4-amino-1,5-dimethyl-2-phenyl-1,2-dihydro-3H-pyrazol-3-one (5) using tin (Sn) and a few drops of concentrated HCl in methanol under reflux conditions for 3–4 hours. The reaction mixture was then cooled, filtered, and the product was isolated and purified by recrystallization. The synthesis of 1,3-diphenyl-1H-pyrazole-4-carbaldehyde derivatives (8a-8j) is depicted in Scheme 1. A mixture of phenyl hydrazine (1) and the corresponding acetophenone derivatives (6a-6j) in methanol was catalyzed by the addition of 2-3 drops of glacial acetic acid. The reaction mixture was stirred at ambient temperature or within the range of 30–40 °C for 2–6 h. Upon completion of the reaction, the mixture was introduced into cold water to facilitate product precipitation. The resultant solid was collected via vacuum filtration, washed with cold water, and purified by recrystallization from ethanol to yield pure (E)-1-phenyl-2-(1-phenylethylidene) hydrazine derivatives (7a-7j).

Phosphorus oxychloride (POCl3) and the specified product were introduced into an anhydrous N,N-dimethylformamide (DMF) solution under a nitrogen atmosphere. The reaction mixture was subjected to reflux at a temperature range of 80–100 °C for 4–6 h. After cooling to ambient temperature, the mixture was transferred onto crushed ice with continuous stirring, resulting in the formation of a precipitate. The solid precipitate was isolated by vacuum filtration, thoroughly washed with water, and subsequently dried. The final product, 1,3-diphenyl-1H-pyrazole-4-carbaldehyde derivatives (8a-8j), was obtained via recrystallization from ethanol. Subsequently, a mixture comprising 4-amino-1,5-dimethyl-2-phenyl-1,2-dihydro-3H-pyrazol-3-one (5) and the 1,3-diphenyl-1H-pyrazole-4-carbaldehyde derivative (8a-8j) was dissolved in 2-methyltetrahydrofuran at room temperature. The reaction mixture was stirred for 40–45 min, and the progress was monitored using thin-layer chromatography (TLC). Upon completion, the reaction mixture was introduced into cold water to precipitate the product. The resulting solid was collected via vacuum filtration, washed with cold water and dried. The crude product, (Z)-4-(((1,3-diphenyl-1H-pyrazol-4-yl) methylene) amino)-1,5-dimethyl-2-phenyl-1,2-dihydro-3H-pyrazol-3-one derivatives (9a-9j), was purified through recrystallization from ethanol. The reaction conditions for the synthesis of 9a were optimized by employing various solvents and adjusting the reaction time. As illustrated in Table 01, 2-methyltetrahydrofuran emerged as the most efficacious solvent among those evaluated, achieving the highest yield of 88% within 40 min. Dimethyl sulfoxide (DMSO) yielded 90% with a reaction duration of 90 min, whereas acetonitrile (ACN) produced an 87% yield in 90 min. Dichloromethane (DCM) resulted in an 80% yield in 65 min, ethanol provided a 78% yield in 60 min, and acetone achieved an 82% yield in 80 min. The yield of the product is contingent on both the reaction time and the solvents employed.

Table 1: Optimization Reaction condition of 9a compound

Sr. No.	Solvent	Time (min)	Yield (%)
1	Dimethyl Sulfoxide (DMSO)	90	90
2	Acetonitrile (ACN)	90	87
3	Dichloromethane (DCM)	65	80
4	2-Methyltetrahydrofuran (2-MeTHF)	40	88
5	Ethanol	60	78
6	Acetone	80	82

[a]All reactions were performed at room temperature.

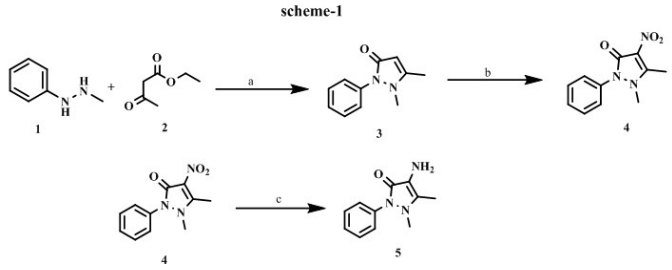

Reagents and conditions: a= Ethanol, reflux 3-4 hr. b = con. HNO_3, glacial acetic acid, 0-5 °C. c = tin, con. HCl, methanol, reflux 3-4 h.

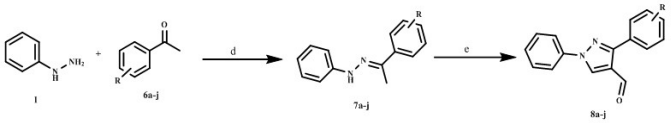

Reagents and conditions: d = methanol, glacial acetic acid, 30-40 °C, 2-6 h; e = DMF, $POCl_3$, 80–100 °C, 4–6 h.

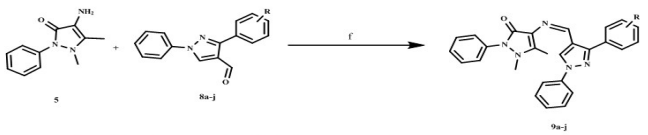

Reagent and condition: f = 2-methyltetrahydrofuran, 40–45 minutes, room temperature.

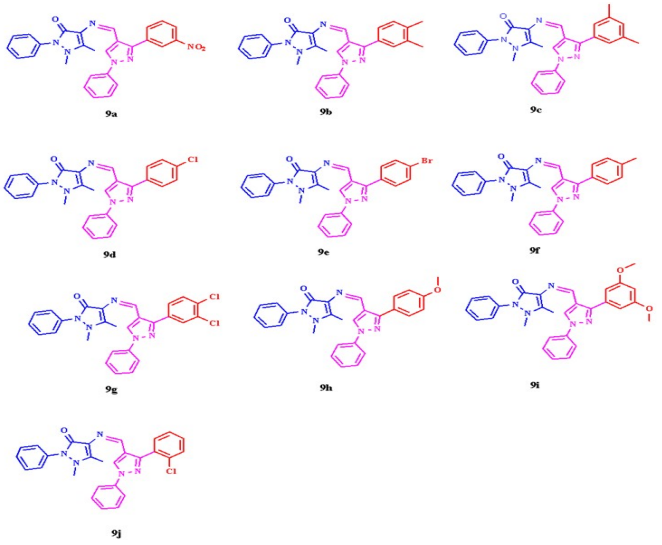

Fig.1. structure of (Z)-4-(((1,3-diphenyl-1*H*-pyrazol-4-yl) methylene) amino)-1,5-dimethyl-2-phenyl-1,2-dihydro -3H-pyrazol-3-one derivatives (9a-9j)

Table 2. Anti-microbial activity of 9a to 9j.values are in (µg/ml)

Compound	*E. coli*	*P. aeruginosa*	*S. aureus*	*B. cereus*	*C. albicans*	*C. tropicalis*
9a	73	58	97	106	124	84
9b	83	44	119	69	123	43
9c	48	79	81	88	70	109
9d	19	16	115	118	22	91
9e	17	23	99	34	72	68
9f	53	30	80	27	63	100
9g	61	21	41	56	26	45
9h	77	120	93	101	25	96
9i	55	46	47	35	50	122
9j	64	42	75	78	111	38
Ampicillin	600	800	600	500	-	-
Nystatin	-	-	-	-	1000	1000

Table 3. Molecular docking analysis of synthesized compounds (9a-j) and Nystatin against Crystal structure of the staphylococcus aureus (3GR6) target protein showing docking scores and detailed protein-ligand interaction profiles

Compound code	Docking score (kcal/mol)	Hydrophobic interactions	Polar interactions	H-bond	Others
9a	-7.068	ILE 14, ILE 20, ILE 94, ILE 102, ILE 120, ILE 193, LEU 102, PRO 192, VAL 201, ALA 15, ALA 95, ALA 97, ALA 190, PHE 96, PHE 204, TYR 147, TYR 157, GLY 13, GLY 191, MET 160	THR 145, THR 146, THR 195, SER 19, SER 93, SER 197	ARG 40 (H-bond sidechain with nitro group O)	LYS 164 (charged positive), ARG 40 (charged positive), Nitro group interactions, Solvent exposure
9b	-7.18	ILE 14, ILE 20, ILE 94, ILE 120, ILE 193, LEU 102, PRO 192, VAL 201, ALA 15, ALA 95, ALA 97, ALA 190, PHE 96, PHE 204, TYR 39, TYR 147, TYR 157, GLY 13, GLY 191, MET 160	THR 145, THR 146, THR 195, SER 19, SER 93, SER 197	-	LYS 164 (charged positive), ARG 40 (charged positive), Solvent exposure
9c	-6.659	ILE 20, ILE 94, ILE 102, ILE 193, ILE 207, LEU 102, LEU 196, PRO 192, VAL 154, VAL 201, ALA 95, ALA 97, ALA 190, PHE 96, PHE 204, TYR 147, TYR 157, GLY 13, GLY 191, GLY 200, MET 160	THR 145, THR 195, SER 19, SER 93, SER 197	-	LYS 164 (charged positive), Pi-Pi stacking (pyrazole-trimethylphenyl), Solvent exposure
9d	-6.968	ILE 14, ILE 20, ILE 94, ILE 207, LEU 102, PRO 192, VAL 201, ALA 15, ALA 95, ALA 96, ALA 97, ALA 198, ALA 190, PHE 96, PHE 204, TYR 147, TYR 157, GLY 13, GLY 191, MET 160	THR 145, THR 146, THR 195, SER 19, SER 93, SER 197	-	LYS 164 (charged positive), ARG 40 (charged positive), Halogen bond (Cl with aromatic ring), Solvent exposure
9e	-6.713	ILE 14, ILE 20, ILE 94, ILE 207, LEU 102, PRO 192, VAL 201, ALA 15, ALA 95, ALA 190, PHE 96, PHE 204, TYR 147, GLY 13, GLY 191, MET 160	THR 145, THR 146, THR 195, SER 93, SER 197	-	LYS 164 (charged positive), ARG 40 (charged positive), Halogen bond (Br with aromatic ring), Solvent exposure
9f	-6.709	ILE 14, ILE 20, ILE 94, ILE 193, ILE 207, LEU 102, PRO 192, VAL 201, ALA 15, ALA 95, ALA 97, ALA 190, PHE 96, PHE 204, TYR 147, TYR 157, GLY 13, GLY 191, MET 160	THR 145, THR 146, THR 195, SER 19, SER 44, SER 93, SER 197	-	LYS 164 (charged positive), ARG 40 (charged positive), Pi-Pi stacking (phenyl rings), Solvent exposure
9g	-6.744	ILE 14, ILE 20, ILE 94, ILE 193, LEU 102, PRO 192, VAL 201, ALA 15, ALA 95, ALA 97, ALA 190, PHE 204, TYR 147, TYR 157, GLY 13, GLY 191, MET 160	THR 145, THR 146, THR 195, SER 19, SER 197	-	LYS 164 (charged positive), ARG 40 (charged positive), Halogen bond (Cl with ARG 40), Solvent exposure
9h	-7.237	ILE 14, ILE 20, ILE 94, LEU 102, PRO 192, VAL 201, ALA 15, ALA 95, ALA 97, ALA 190, PHE 96, PHE 204, TYR 39, TYR 147, TYR 157, GLY 13, GLY 191, MET 160	THR 145, THR 146, THR 195, SER 19, SER 44, SER 93, SER 197	SER 197 (H-bond with pyrazole N)	LYS 41, LYS 164 (charged positive), ARG 40 (charged positive), Solvent exposure
9i	-6.162	ILE 14, ILE 20, ILE 94, ILE 193, LEU 102, PRO 192, VAL 201, ALA 15, ALA 97, ALA 190, PHE 96, PHE 204, TYR 147, TYR 157, GLY 13, GLY 191, GLY 200	THR 145, THR 146, THR 195, SER 93, SER 197	-	LYS 41, LYS 164 (charged positive), ARG 40 (charged positive), Solvent exposure
9j	-7.2	ILE 14, ILE 20, ILE 94, ILE 207, LEU 102, PRO 192, VAL 201, ALA 15, ALA 95, ALA 97, ALA 190, ALA 198, PHE 96, PHE 204, TYR 147, TYR 157, GLY 13, GLY 191, GLY 200, MET 160	THR 145, THR 146, THR 195, SER 19, SER 93, SER 197	SER 197 (H-bond with pyrazole N)	LYS 164 (charged positive), Halogen bond (Cl with pyrazole ring), Solvent exposure
Nystatin	-4.073	LEU 52, LEU 62, PRO 58, ALA 60, TYR 39, TYR 63, HIS 61	GLN 57, SER (multiple OH groups on polyene)	Multiple H-bonds with hydroxyl groups on the macrolide ring to GLU 42, GLU 49, GLU 53, GLU 59, LYS 46, LYS 50, ARG 45	GLU 42, GLU 49, GLU 53, GLU 59 (charged negative), LYS 46, LYS 50 (charged positive), ARG 45 (charged positive), Complex macrolide-protein interactions, Extensive hydrogen bonding network, Solvent exposure

Biological Activity: All the newly synthesized compounds were screened for their antimicrobial activity. For the Antimicrobial studies 4 bacterial strains (*S. aureus* MTCC 2408, *B. cereus* MTCC430, *E. coli* MTCC 2412 and *P. aeruginosa* MTCC 2081) and 2 fungal strains (*C. albicans* MTCC 227and *C. tropicalis* MTCC 230) were used. Antimicrobial study was assessed by Minimum Inhibitory concentration (MIC) by serial dilution method. Results indicate that, most of the synthesized compounds have shown good to moderate activity against *S. aureus, B. cereus, E. coli* and *P. aeruginosa* bacterial strain. In particular, compound 9e, 9d has exhibited excellent activity against *E. coli* and *P. aeruginosa* whereas 9g and 9fgives better inhibition of *B. cereus* and *S. auerus*. Overall, pyrazole derived Schiff bases show good inhibition against both gram negative and gram-positive bacterial strains. Overall, the variation in compound structure, associated side chains tend to work differently for bacterial inhibition. Different published reports pave a path to understand variation in the inhibitory activity. The lipophilic nature of compounds, presence of the enzyme inhibitors (for e.g. DNA gyrase), and chelating activity due to presence of metal ions contributes to different inhibitory action against bacterial species(5, 12, 13). For Antifungal studies, the compounds 9d and 9j displayed better inhibitory activity against *C. albicans* and *C. tropicalis*. The antifungal inhibition by pyrazole derived Schiff bases can be attributed due to its ability to inhibit biofilm formation and also interference in nucleic acid synthesis of fungal strains(14, 15).

Molecular docking: Molecular docking analysis was performed to evaluate the binding affinity and interaction patterns of synthesized compounds 9a-9j with the Crystal structure of the Staphylococcus aureus (3GR6) target protein. Nystatin, a clinically used polyene antifungal agent, served as the reference standard. The docking scores ranged from -6.162 to -7.237 kcal/mol for the synthesized compounds, demonstrating significantly superior binding affinity compared to Nystatin (-4.073 kcal/mol). Compound 9h exhibited the highest binding affinity (-7.237 kcal/mol), followed by 9j (-7.2 kcal/mol), 9b (-7.18 kcal/mol), and 9a (-7.068 kcal/mol). Notably, all synthesized compounds demonstrated 1.5-3.1 kcal/mol better binding energy than Nystatin, suggesting enhanced interaction with the target protein and potential improved antifungal efficacy. The binding mode analysis revealed that all compounds 9a-j occupied a conserved hydrophobic pocket formed by ILE 14, ILE 20, ILE 94, PRO 192, ALA 190, PHE 204, GLY 13, GLY 191, and MET 160. This extensive hydrophobic network appeared critical for ligand stabilization. Polar interactions were consistently established with THR 145, THR 146, THR 195, SER 93, and SER 197, while positively charged residues LYS 164 and ARG 40 provided electrostatic stabilization across all compounds. Hydrogen bonding analysis identified distinct patterns. Compounds 9a, 9h, and 9j formed specific H-bonds: 9a through ARG 40 with the nitro group oxygen, while both 9h and 9j established H-bonds via SER 197 with the pyrazole nitrogen. These specific hydrogen bonding interactions correlated strongly with enhanced binding affinity, as evidenced by the top three docking scores.

Experimental: Commercially available reagents and solvents from Sigma–Aldrich, Avra, or Spectrochem were utilized without additional purification. The melting points were determined in open glass capillary tubes using a Stuart SMP3 apparatus and are uncorrected. The IR spectra were recorded on a Shimadzu IR Affinity-1 spectrometer. The ^{1}H and ^{13}C NMR spectra were measured on a Bruker spectrometer at 400 and 100 MHz, respectively. The mass spectra were obtained with a Shimadzu GCMS-QP-2010 Ultra instrument equipped with an electron ionization source, a quadrupole detector, and a direct inlet probe method. Thin layer chromatography (TLC) was executed on 5 × 20- cm plates coated with a 0.25-mm layer of Silica gel 60 F254 (Merck); when required, visualization was carried out using suitable agents.

General Synthesis of 1,5-Dimethyl-2-phenyl-1,2-dihydro-3H-pyrazol-3-one (3): A solution comprising phenyl hydrazine (1) and ethyl 3-oxobutanoate (2) was prepared in ethanol, to which 2–3 drops of acetic acid were introduced to act as a catalyst. The reaction mixture was subsequently subjected to reflux heating for a duration of 3–4 hours to promote condensation and subsequent cyclization. Upon completion of the reaction, the mixture was allowed to cool to ambient temperature, resulting in the formation of a solid product. The crude product, 1,5-Dimethyl-2-phenyl-1,2-dihydro-3H-pyrazol-3-one (3), was isolated by filtration and washed with cold ethanol to eliminate impurities.

General Synthesis of 1,5-dimethyl-4-nitro-2-phenyl-1,2-dihydro-3H-pyrazol-3-one (4): The compound 1,5-Dimethyl-2-phenyl-1,2-dihydro-3H-pyrazol-3-one (**3**) was nitrated using concentrated nitric acid in glacial acetic acid. The reaction was conducted at a temperature range of 0–5 °C with continuous stirring, after which it was allowed to reach ambient temperature. Upon completion, the reaction mixture was introduced into ice water to facilitate product precipitation. The precipitate was subsequently filtered, washed, and recrystallized. This process results in the formation of 1,5-dimethyl-4-nitro-2-phenyl-1,2-dihydro-3H-pyrazol-3-one (**4**) via electrophilic substitution at the 4-position.

General Synthesis of 4-amino-1,5-dimethyl-2-phenyl-1,2-dihydro-3H-pyrazol-3-one (5): The compound 1,5-Dimethyl-4-nitro-2-phenyl-1,2-dihydro-3H-pyrazol-3-one (4) undergoes reduction to form 4-amino-1,5-dimethyl-2-phenyl-1,2-dihydro-3H-pyrazol-3-one (5) through the use of tin (Sn) and a few drops of concentrated hydrochloric acid (HCl) in methanol under reflux conditions for a duration of 3–4 hours. After cooling the reaction mixture, filtration was performed, and the product was subsequently isolated and purified via recrystallization. This procedure effectively transforms the nitro group at position 4 into an amine group.

General Procedure for the Synthesis of (E)-1-Phenyl-2-(1-phenylethylidene) hydrazine Derivatives (7a-7j): Phenylhydrazine (**1**) and the corresponding acetophenone derivatives (**6a-6j**) were dissolved in methanol, and 2–3 drops of glacial acetic acid were added. The reaction mixture was stirred at room temperature or at 30–40 °C for 2–6 hours, and the progress was monitored by thin-layer chromatography (TLC). Upon completion, the reaction mixture was poured into cold water, resulting in the precipitation of the product. The solid was collected by vacuum filtration, washed with cold water, and purified by recrystallization from ethanol to afford the pure (E)-1-phenyl-2-(1-phenylethylidene) hydrazine derivatives (7a-7j).

General Procedure for the Synthesis of 1,3-Diphenyl-1H-pyrazole-4-carbaldehyde Derivatives (8a-8j): A mixture of (E)-1-phenyl-2-(1-phenylethylidene) hydrazine derivatives (7a-7j) and phosphorus oxychloride ($POCl_3$) was added to dry N,N-dimethylformamide (DMF) under a nitrogen atmosphere. The reaction mixture was refluxed at 80–100 °C for 4–6 hours, and the progress was monitored by thin-layer chromatography (TLC). Upon completion, the reaction mixture was cooled to room temperature and carefully poured onto crushed ice with stirring. The resulting precipitate was collected by vacuum filtration, washed thoroughly with water, and dried. The crude product 1,3-diphenyl-1*H*-pyrazole-4-carbaldehyde derivatives (8a-8j)was purified by recrystallization from ethanol.

General Procedure for the Synthesis of (Z)-4-(((1,3-diphenyl-1H-pyrazol-4-yl) methylene) amino)-1,5-dimethyl-2-phenyl-1,2-dihydro-3H-pyrazol-3-one Derivatives (9a-9j): A solution was prepared by dissolving a mixture of 4-amino-1,5-dimethyl-2-phenyl-1,2-dihydro-3H-pyrazol-3-one (5) and the 1,3-diphenyl-1H-pyrazole-4-carbaldehyde derivative (8a-8j) in 2-methyltetrahydrofuran at ambient temperature. The reaction mixture was stirred for 40–45 min, and its progress was monitored using thin-layer chromatography (TLC). Upon completion, the reaction mixture was introduced into cold water to facilitate product precipitation. The resulting solid was collected via vacuum filtration, washed with cold water, and dried. The crude product, identified as (Z)-4-(((1,3-diphenyl-1H-pyrazol-4-yl) methylene) amino)-1,5-dimethyl-2-phenyl-1,2-dihydro-3H-pyrazol-3-one derivatives (9a-9j), underwent purification through recrystallization from ethanol.

(Z)-1,5-dimethyl-4-(((3-(3-nitrophenyl)-1-phenyl-1H-pyrazol-4-yl) methylene) amino)-2-phenyl-1,2-dihydro-3H-pyrazol-3-one(9a). Yield 88%, dark yellow solid, 240-242 °C.IR spectrum (KBr), ν, cm^{-}

[1]: 3150, 3000, 1715, 1690, 1550, 690.[1]H NMR spectrum(500 MHz, DMSO-d_6) 8.74 (1 H, s), 8.70 (1 H, s), 8.65 (1 H, t, *J* 2.1), 8.14 (1 H, ddd, *J* 8.6, 2.0, 1.1), 8.09 (1 H, ddd, *J* 7.9, 2.2, 1.2), 8.05 – 7.99 (2 H, m), 7.69 (1 H, dd, *J* 8.7, 7.9), 7.56 – 7.48 (4 H, m), 7.48 – 7.42 (1 H, m), 7.41 – 7.35 (2 H, m), 7.35 – 7.30 (1 H, m). ^{13}C NMR spectrum (125 MHz, DMSO-d_6) 146.24, 138.75, 131.76, 130.00, 129.60, 129.28, 127.52, 126.96, 126.41, 125.81, 125.22, 119.45, 34.48, 12.81. Mass spectrum: m/z 479.30 $(M+H)^+$ $C_{27}H_{22}N_6O_3$. M 478.18.

(Z)-4-(((3-(3,5-dimethylphenyl)-1-phenyl-1H-pyrazol-4-yl) methylene) amino)-1,5-dimethyl-2-phenyl-1,2-dihydro-3H-pyrazol-3-one (9c). Yield 84%, pale yellow solid, mp 238-240°C. 7.36 (3 H, m), 7.36 – 7.32 (2 H, m), 7.32 – 7.26 (1 H, m), 3.17 (3 H, s), 2.23 (3 H, d, *J* 0.9), 2.19 (3 H, d, *J* 1.9). ^{13}C NMR spectrum (125 MHz, DMSO-d_6) 146.24, 138.75, 133.08, 131.15, 129.60, 129.28, 127.52, 126.96, 126.00, 125.22, 119.45, 34.48, 19.97, 19.80, 12.81. Mass spectrum: m/z 462.2 $(M+H)^+$ $C_{29}H_{27}N_5O$. M 461.2.

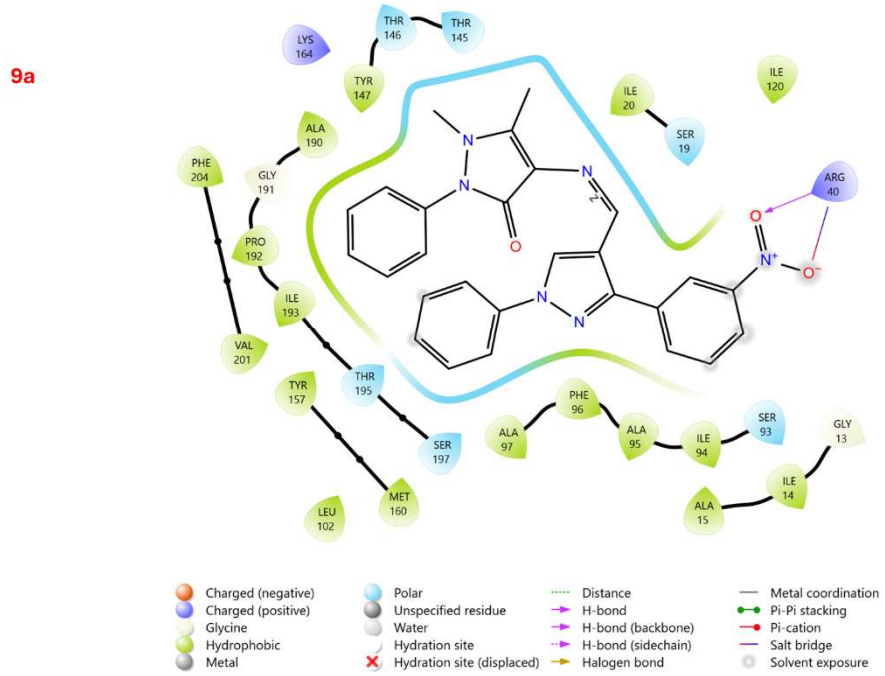

Figure 01. 2D interaction maps of compounds 9a and Nystatin against the crystal structure of the Staphylococcus aureus (3GR6) target protein, showing docking scores and detailed protein-ligand interaction profiles

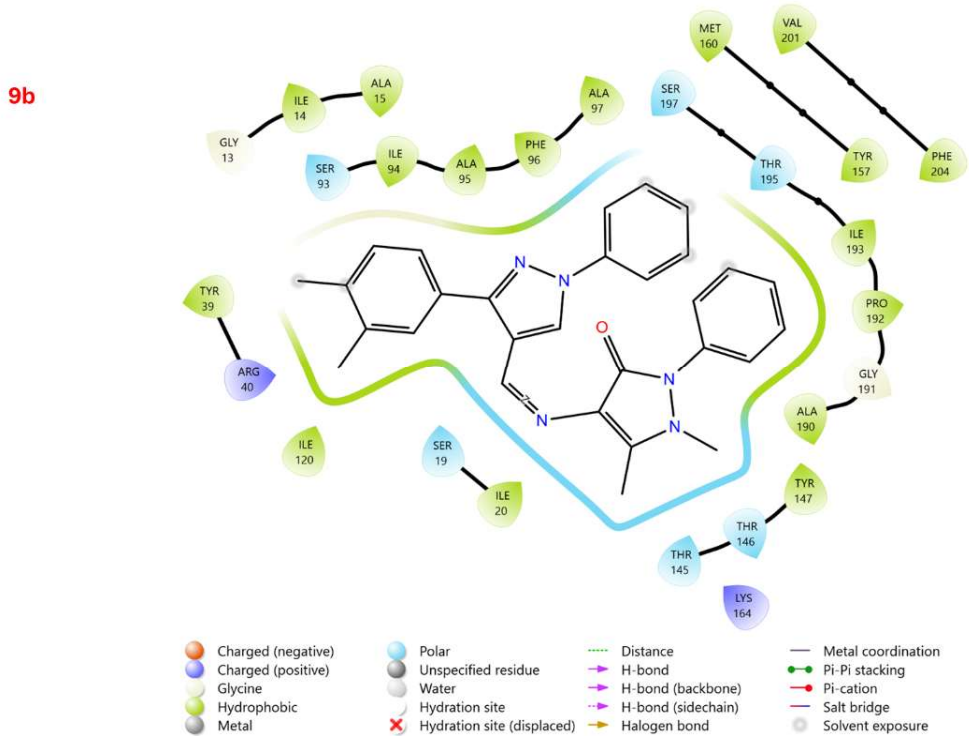

Figure 02. 2D interaction maps of compounds 9b and Nystatin against the crystal structure of the Staphylococcus aureus (3GR6) target protein, showing docking scores and detailed protein-ligand interaction profiles

(Z)-4-(((3-(3,4-dimethylphenyl)-1-phenyl-1H-pyrazol-4-yl) methylene) amino)-1,5-dimethyl-2-phenyl-1,2-dihydro-3H-pyrazol-3-one (9b). Yield 83%, light orange solid, mp 235-237°C. IR spectrum (KBr), ν, cm^{-1}: 3150, 3010, 1720, 1680, 1640, 1450, 680. ^{1}H NMR spectrum (500 MHz, DMSO-d_6) 8.74 (1 H, s), 8.70 (1 H, s), 8.05 – 7.99 (2 H, m), 7.67 (1 H, d, *J* 2.0), 7.56 – 7.42 (5 H, m), 7.41 – IR spectrum (KBr), ν, cm^{-1}: 3150, 3050, 1725, 1690, 1650, 1450, 690. ^{1}H NMR spectrum (500 MHz, DMSO-d_6) 8.74 (1 H, s), 8.70 (1 H, s), 8.05 – 7.99 (2 H, m), 7.56 – 7.42 (5 H, m), 7.41 – 7.30 (3 H, m), 7.04 (2 H, d, *J* 2.1), 6.92 – 6.88 (1 H, m), 3.17 (3 H, s), 2.44 (3 H, s), 2.09 (6 H, d, *J* 1.8).^{13}C NMR spectrum (125 MHz, DMSO-d_6) 146.24, 138.75, 132.99, 129.60, 129.28, 127.52, 127.01 (d, *J* 14.1),

125.22, 119.45, 34.48, 21.13, 12.81. Mass spectrum: m/z 462.2 $(M+H)^+$ $C_{29}H_{27}N_5O$. M 461.2.

(Z)-4-(((3-(4-chlorophenyl)-1-phenyl-1H-pyrazol-4-yl) methylene) amino)-1,5-dimethyl-2-phenyl-1,2-dihydro-3H-pyrazol-3-one (9d). Yield 78%, deep yellow solid, mp 248-250°C. IR spectrum (KBr), ν, cm^{-1}: 3140, 3000, 1714, 1691, 1650, 1430, 785, 690.^{1}H NMR spectrum(500 MHz, DMSO-d_6) 8.74 (1 H, s), 8.70 (1 H, s), 8.05 – 7.99 (2 H, m), 7.90 – 7.84 (2 H, m), 7.54 – 7.42 (7 H, m), 7.41 – 7.35 (2 H, m), 7.35 – 7.30 (1 H, m). ^{13}C NMR spectrum (125 MHz, DMSO-d_6) 146.24, 138.75, 130.44, 129.60, 129.28, 128.88, 127.52, 126.96, 125.22, 119.45, 34.48, 12.81. Mass spectrum: m/z 469.15 $(M+H)^{+2}$ $C_{27}H_{22}ClN_5O$. M 467.15.

(Z)-4-(((3-(4-bromophenyl)-1-phenyl-1H-pyrazol-4-yl) methylene) amino)-1,5-dimethyl-2-phenyl-1,2-dihydro-3H-pyrazol-3-one(9e). Yield 80%, light yellow solid, mp 243-245°C. IR spectrum (KBr), ν, cm^{-1}: 3150, 3090, 1715, 1695, 1645, 1450, 667, 690.^{1}H NMR spectrum (500 MHz, DMSO-d_6) 8.74 (1 H, s), 8.70 (1 H, s), 8.05 – 7.99 (2 H, m), 7.86 – 7.80 (2 H, m), 7.61 – 7.55 (2 H, m), 7.55 – 7.48 (4 H, m), 7.48 – 7.42 (1 H, m), 7.41 – 7.35 (2 H, m), 7.35 – 7.30 (1 H, m). ^{13}C NMR spectrum (125 MHz, DMSO-d_6) 146.24, 138.75, 131.60, 129.85, 129.60, 129.28, 127.52, 126.96, 125.22, 119.45, 34.48, 12.81. Mass spectrum: m/z 513.10 $(M+H)^+$ $C_{27}H_{22}BrN_5O$. M 511.10.

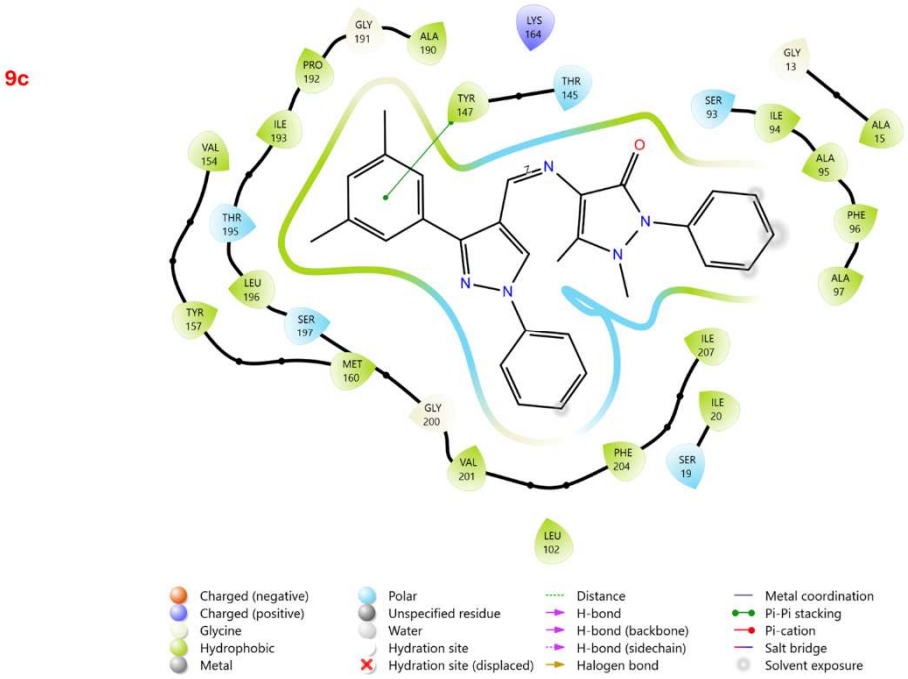

Figure 3. 2D interaction maps of compounds 9c and Nystatin against the crystal structure of the Staphylococcus aureus (3GR6) target protein, showing docking scores and detailed protein-ligand interaction profiles

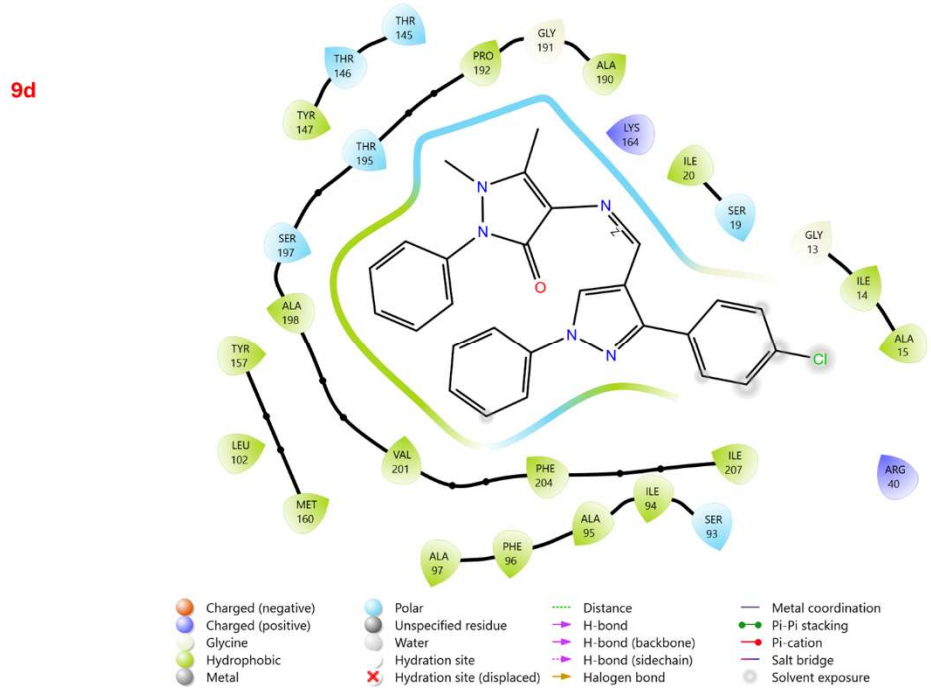

Figure 04. 2D interaction maps of compounds 9d and Nystatin against the crystal structure of the Staphylococcus aureus (3GR6) target protein, showing docking scores and detailed protein-ligand interaction profiles

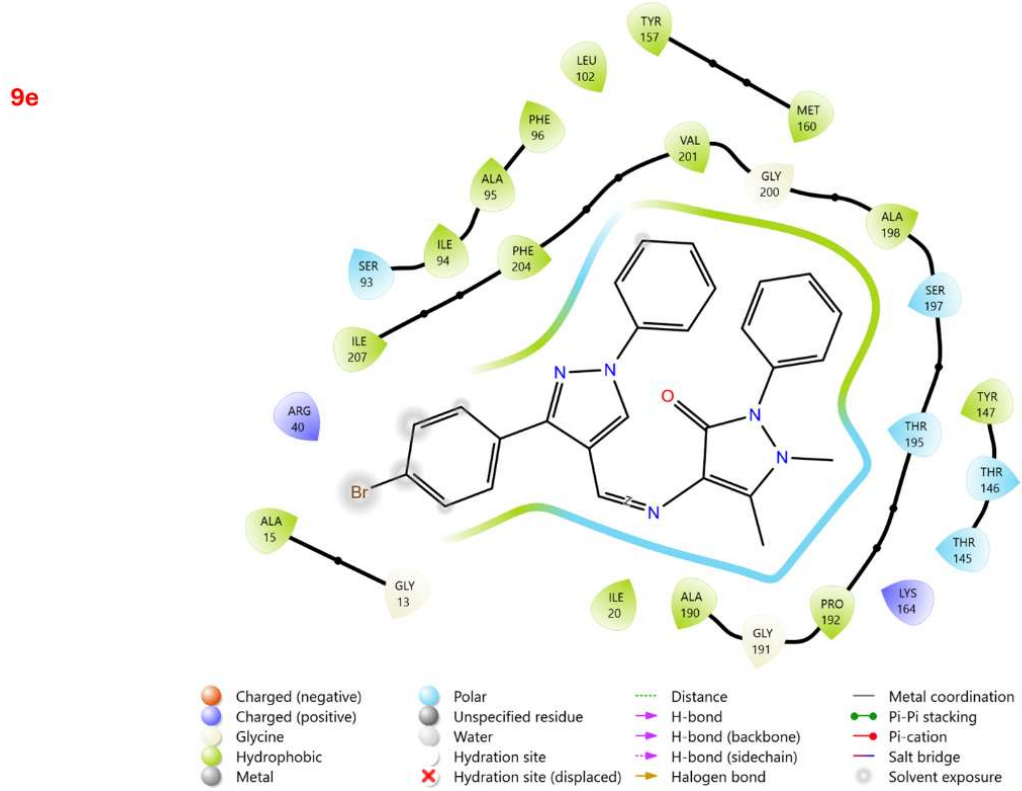

Figure 5. 2D interaction maps of compounds 9e and Nystatin against the crystal structure of the Staphylococcus aureus (3GR6) target protein, showing docking scores and detailed protein-ligand interaction profiles

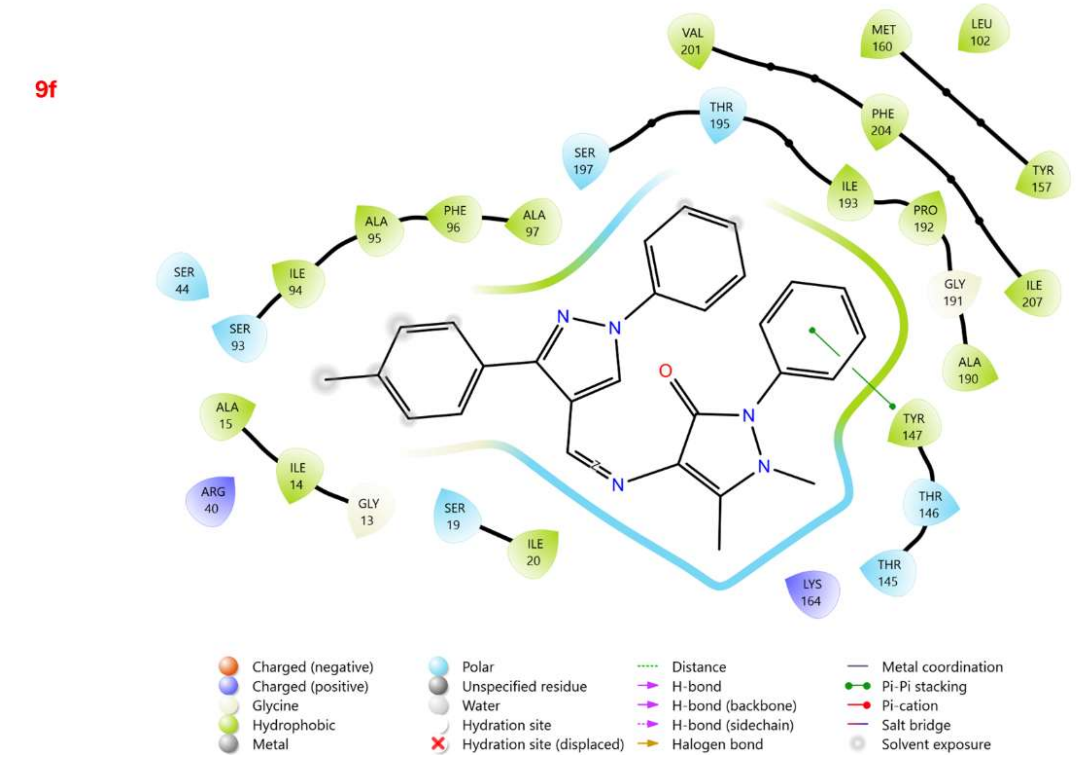

Figure 6. 2D interaction maps of compounds 9f and Nystatin against the crystal structure of the Staphylococcus aureus (3GR6) target protein, showing docking scores and detailed protein-ligand interaction profiles

(Z)-1,5-dimethyl-2-phenyl-4-(((1-phenyl-3-(p-tolyl)-1H-pyrazol-4-yl) methylene) amino)-1,2-dihydro-3H-pyrazol-3-one (9f). Yield 86%, light yellow solid, mp 239-241°C. IR spectrum (KBr), ν, cm^{-1}: 3140, 3020, 1712, 1680, 1620, 1415, 691. ^{1}H NMR spectrum (500 MHz, DMSO-d_6) 8.74 (1 H, s), 8.70 (1 H, s), 8.05 – 7.99 (2 H, m), 7.56 – 7.42 (7 H, m), 7.41 – 7.35 (2 H, m), 7.35 – 7.30 (1 H, m), 7.24 – 7.18 (2 H, m), 2.32 (3 H, d, *J* 0.9). ^{13}C NMR spectrum (125 MHz, DMSO-d_6) 146.24, 138.75, 129.60, 129.29, 129.04, 127.52, 126.96, 125.22, 119.45, 34.48, 21.42, 12.81. Mass spectrum: m/z 448.21 $(M+H)^+$ $C_{28}H_{25}N_5O$. M 447.21.

(Z)-4-(((3-(3,4-dichlorophenyl)-1-phenyl-1H-pyrazol-4-yl) methylene) amino)-1,5-dimethyl-2-phenyl-1,2-dihydro-3H-pyrazol-3-one (9g). Yield 81%, pale yellow solid, mp 236-238°C. IR

spectrum (KBr), ν, cm^{-1}: 3150, 3060, 1716, 1692, 1640, 1450, 785, 780, 540.^{1}H NMR spectrum (500 MHz, DMSO-d_6) 8.74 (1 H, s), 8.70 (1 H, s), 8.05 – 7.99 (2 H, m), 7.75 (1 H, dd, *J* 8.6, 2.2), 7.62 (1 H, d, *J* 2.2), 7.56 – 7.49 (4 H, m), 7.49 – 7.42 (1 H, m), 7.41 – 7.35 (2 H, m), 7.35 – 7.30 (1 H, m), 7.26 (1 H, d, *J* 8.7). ^{13}C NMR spectrum (125 MHz, DMSO-d_6) 146.24, 138.75, 131.19, 129.60, 129.28, 128.93, 128.18, 127.52, 126.96, 125.22, 119.45, 34.48, 12.81. Mass spectrum: m/z 503.11 $(M+H)^+$ $C_{27}H_{21}Cl_2N_5O$. M 501.11.

– 6.94 (2 H, m), 3.81 (3 H, s). ^{13}C NMR spectrum (125 MHz, DMSO-d_6) 146.24, 138.75, 130.16, 129.60, 129.28, 127.52, 126.96, 125.22, 119.45, 114.34, 55.35, 34.48, 12.81. Mass spectrum: m/z 464.54 $(M+H)^+$ $C_{28}H_{25}N_5O_2$. M 463.20.

(Z)-4-(((3-(3,5-dimethoxyphenyl)-1-phenyl-1H-pyrazol-4-yl) methylene) amino)-1,5-dimethyl-2-phenyl-1,2-dihydro-3H-pyrazol-3-one (9i). Yield 79%, light yellow solid, mp 246-248. IR

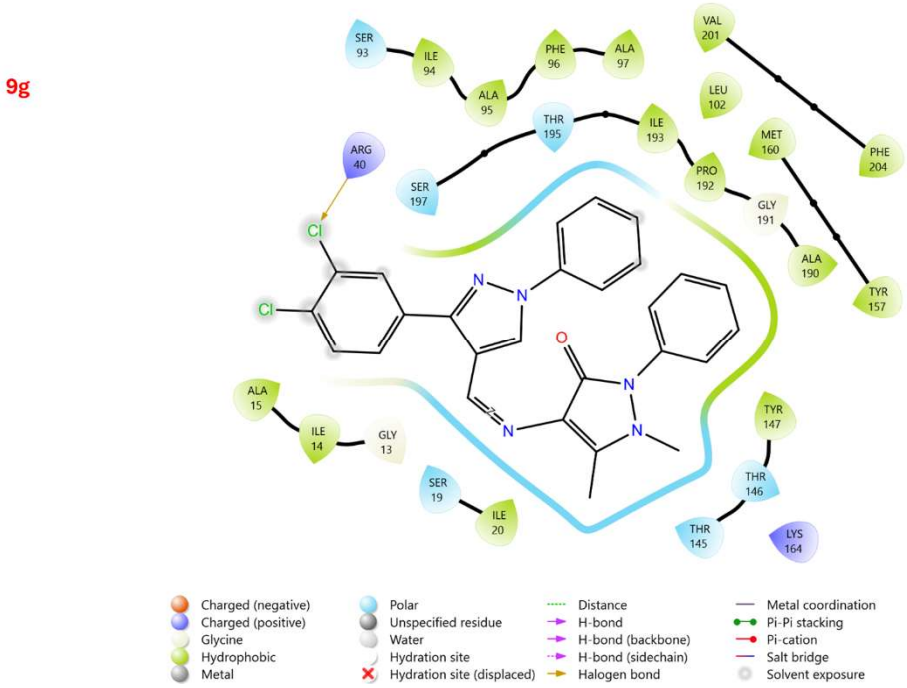

Figure 7. 2D interaction maps of compounds 9g and Nystatin against the crystal structure of the Staphylococcus aureus (3GR6) target protein, showing docking scores and detailed protein-ligand interaction profiles

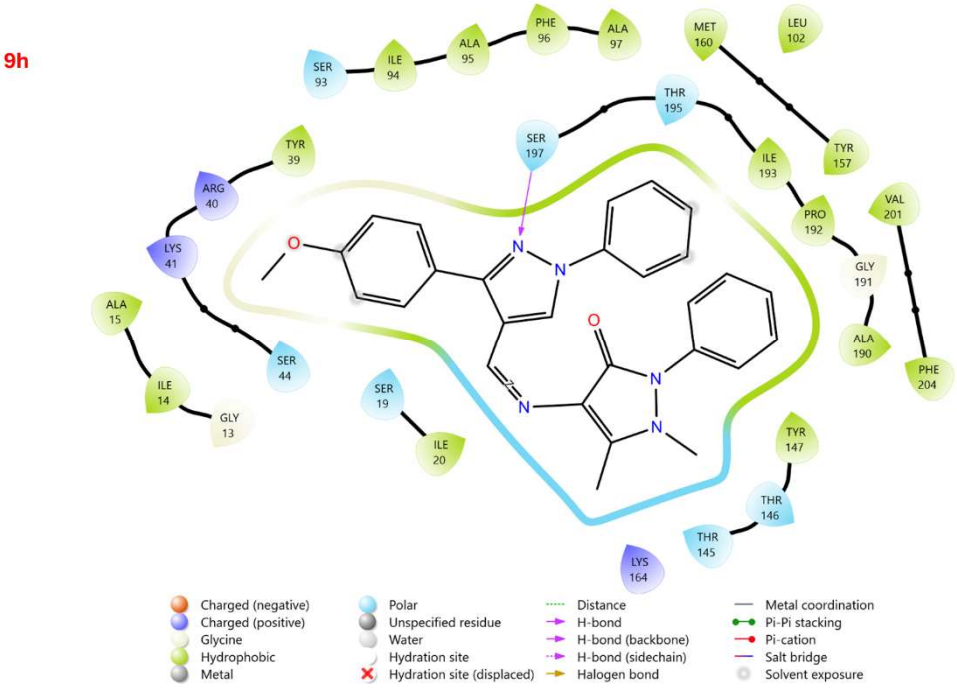

Figure 8. 2D interaction maps of compounds 9h and Nystatin against the crystal structure of the Staphylococcus aureus (3GR6) target protein, showing docking scores and detailed protein-ligand interaction profiles

(Z)-4-(((3-(4-methoxyphenyl)-1-phenyl-1H-pyrazol-4-yl) methylene) amino)-1,5-dimethyl-2-phenyl-1,2-dihydro-3H-pyrazol-3-one (9h.) Yield 82%, light orange solid, mp 244-246°C. IR spectrum (KBr), ν, cm^{-1}: 3150, 3010, 1719, 1690, 1450, 1300, 1100, 690.^{1}H NMR spectrum(500 MHz, DMSO-d_6) 8.74 (1 H, s), 8.70 (1 H, s), 8.05 – 7.99 (2 H, m), 7.64 – 7.58 (2 H, m), 7.56 – 7.48 (4 H, m), 7.48 – 7.42 (1 H, m), 7.41 – 7.35 (2 H, m), 7.35 – 7.30 (1 H, m), 7.00

spectrum (KBr), ν, cm^{-1}: 3160, 3000, 1715, 1690, 1650, 1450, 1300, 1100, 1000, 690.^{1}H NMR spectrum (500 MHz, DMSO-d_6) 8.74 (1 H, s), 8.70 (1 H, s), 8.05 – 7.99 (2 H, m), 7.56 – 7.48 (4 H, m), 7.48 – 7.42 (1 H, m), 7.41 – 7.30 (3 H, m), 6.66 (1 H, t, *J* 2.2), 6.61 (2 H, d, *J* 2.1), 3.85 (6 H, s). ^{13}C NMR spectrum (125 MHz, DMSO-d_6) 146.24, 138.75, 129.60, 129.28, 127.52, 126.96, 125.22, 119.45,

110.32, 103.88, 55.81, 34.48, 12.81. Mass spectrum: m/z 494.21 $(M+H)^+$ $C_{29}H_{27}N_5O_3$, M 493.21.

(Z)-4-(((3-(2-chlorophenyl)-1-phenyl-1H-pyrazol-4-yl) methylene) amino)-1,5-dimethyl-2-phenyl-1,2-dihydro-3H-pyrazol-3-one (9j). Yield 77%, light orange solid, mp 247-249°C. IR spectrum (KBr), ν, cm^{-1}: 3150, 3020, 1716, 1670, 1650, 1450, 785, 690. ^1H NMR spectrum (500 MHz, DMSO-d_6) 8.74 (1 H, s), 8.70 (1 H, s), 8.05 – 7.99 (2 H, m), 7.56 – 7.30 (12 H, m). ^{13}C NMR spectrum (125 MHz, DMSO-d_6) 146.24, 138.27, 130.95, 130.53, 130.00, 129.60, 129.28, 127.52, 127.29, 126.96, 125.22, 119.45, 34.48, 12.81. Mass spectrum: m/z 469.15 $(M+H)^{+2}$ $C_{27}H_{22}ClN_5O$, M 467.15.

Anti-microbial activity and Molecular Docking: The microbial potential of the synthesized organic molecules derivatives is evaluated against gram-positive (*B. cereus and S. aureus*), and gram-negative (*E. coli and P. aerugionosa*) bacteria and, pathogenic fungus (*Candida albicans* and *Candida Tropicalis*). The minimum inhibitory concentration (MIC) is analysed by the micro-broth dilution method using a micro-titer plate. All bacterial strains used for the study is of the mid-log growth phase. Activated broths were reaped through centrifugation and washed with sodium phosphate buffer (10 mM) before mixing with 0.03% muller hilton broth at the desired concentration. Furthermore, the serial dilutions of synthesized derivatives is carried out with muller hilton (50 µL) to attain the

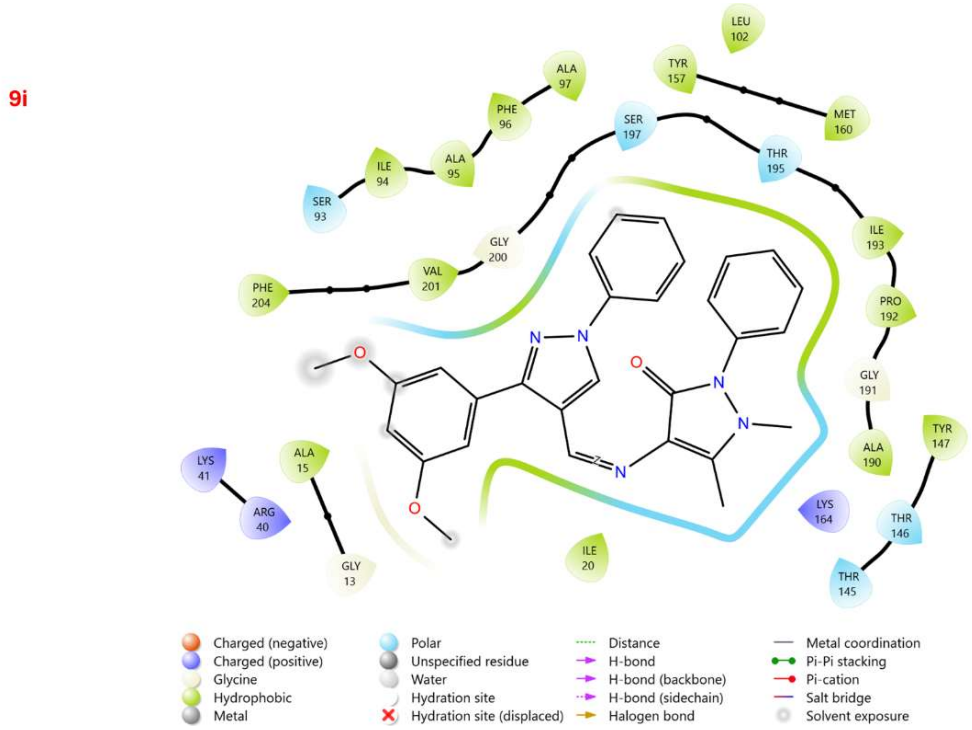

Figure 09. 2D interaction maps of compounds 9i and Nystatin against the crystal structure of the Staphylococcus aureus (3GR6) target protein, showing docking scores and detailed protein-ligand interaction profiles

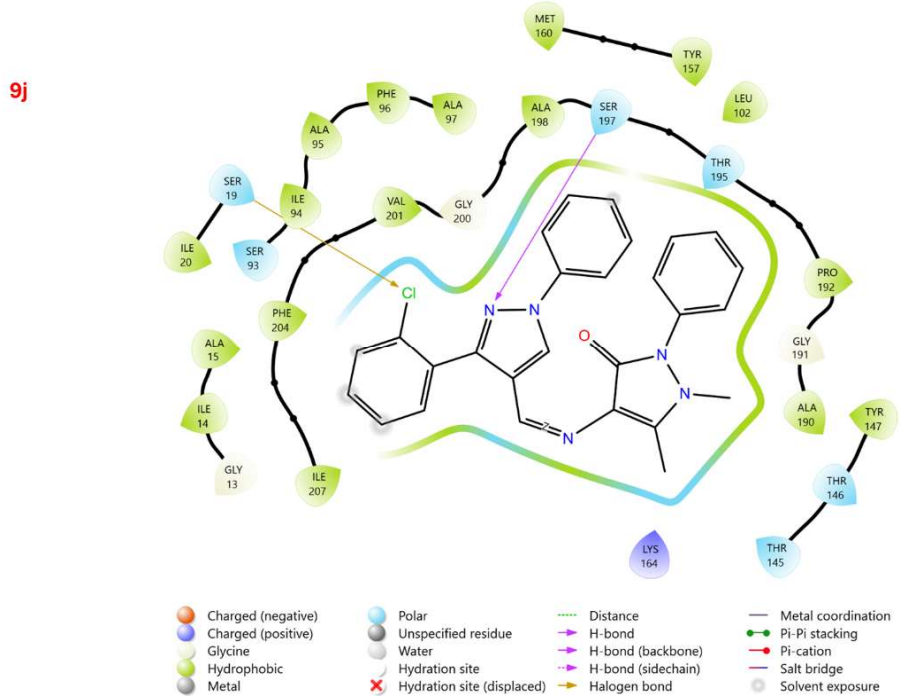

Figure 10. 2D interaction maps of compounds 9j and Nystatin against the crystal structure of the Staphylococcus aureus (3GR6) target protein, showing docking scores and detailed protein-ligand interaction profiles

desired concentrations (20–200 µg/mL) in a 96-well microtiter plate, and then bacterial inoculum (5 × 104 CFU) was inoculated into each well. Finally, the MIC value is determined as the minimum synthesized derivatives and nanoparticles concentration that inhibits the growth of bacterial strains post-incubation of microtiter plates at 37 °C overnight. Molecular docking simulations were performed using the Schrödinger Suite (Schrödinger, LLC, New York, NY) to evaluate the binding interactions of synthesized compounds 9a-9j with antifungal targets.

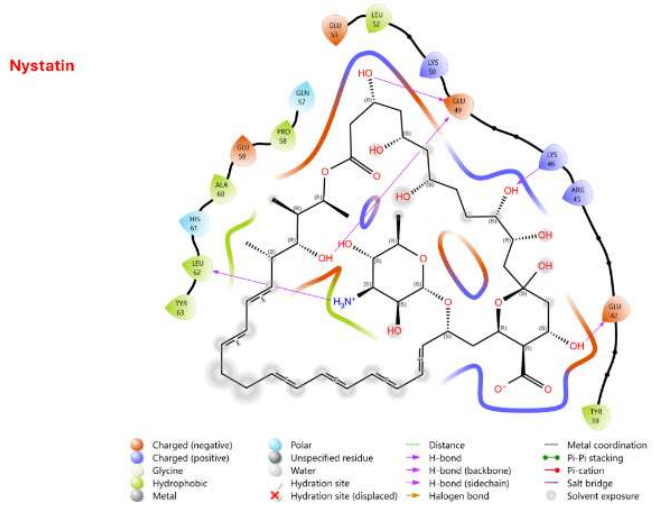

Figure 11. 2D interaction maps of compounds (9a-j) and Nystatin against the crystal structure of the Staphylococcus aureus (3GR6) target protein, showing docking scores and detailed protein-ligand interaction profiles

The Crystal structure of the Staphylococcus aureus (3GR6) was retrieved from the RCSB Protein Data Bank (www.rcsb.org). Protein preparation was conducted using the Protein Preparation Wizard, including removal of water molecules beyond 5 Å, addition of hydrogen atoms, assignment of bond orders, hydrogen bond network optimization using PROPKA at pH 7.0, and energy minimization with the OPLS4 force field (RMSD convergence: 0.30 Å). Ligand structures of compounds 9a-9j and the reference drug Nystatin were prepared using LigPrep module, generating ionization states at pH 7.4 ± 2.0 and optimizing geometries. Receptor grids were generated centered on the active binding site with dimensions of 20 Å × 20 Å × 20 Å. Molecular docking was performed using Glide in extra precision (XP) mode. Binding energies (kcal/mol), RMSD values (threshold: 2.0 Å), and protein-ligand interactions, including hydrogen bonds, hydrophobic contacts, π–π stacking, and halogen bonds, were analysed and visualised using the Maestro interface.

CONCLUSION

This research effectively illustrates the implementation of sustainable techniques in synthesizing (Z)-4-(((1,3-diphenyl-1H-pyrazol-4-yl) methylene) amino)-1,5-dimethyl-2-phenyl-1,2-dihydro-3H-pyrazol-3-one derivatives (9a-9j), in alignment with green chemistry principles to reduce environmental impact. The solvent 2-methyltetrahydrofuran was identified as the most effective, providing high yields and demonstrating the practicality of eco-friendly synthetic methods. This study highlights the critical role of incorporating green chemistry approaches into medicinal chemistry to enhance the sustainability and efficiency of drug development and address both ecological and therapeutic concerns.

This study evaluated the antimicrobial potential of synthetic organic molecule derivatives against pathogenic fungi, gram-positive bacteria, and gram-negative bacteria. The microbroth dilution method was used todetermine the minimum inhibitory concentration (MIC). Muller-Hilton broth was mixed with activated broths, serial dilutions were conducted, and bacterial inoculum was added. After incubation at 37°C overnight, the MIC was calculated. Additionally, molecular docking studies were performed to evaluate the binding affinity and interaction patterns of the synthesized compounds (9a-9j) with the crystal structure of the Staphylococcus aureus target protein (3GR6).

REFERENCES

Aboli sapkal, Santhosh kamble, ChemistrySelect Vol. 5, Issue 42, 2020, pp. 12971-13026,https://doi.org/10.1002/slct.202003008

Lang, Damanpreet K., Kaur, Rajwinder, Arora, Rashmi, Saini, Balraj, Arora, Sandeep, Vol. 20, N0.18, 2020, pp. 2150-2168(19), Bentham Science, https://doi.org/10.2174/1871520620070521491 7

Patki, A. S., Pande, P. R., & Muley, D. B., *Development of New Method for the Synthesis of Pyrazole Derivative*, IJARSCT, 2023, pp. 122–125.https://doi.org/10.48175/IJARSCT-8125

bhupender Nehra, Sandeep Rulhania, Shalini Jaswal, Bhupinder Kumar, Gurpreet Singh, Vikramdeep Monga, European Journal of Medicinal Chemistry, Vol. 205, 1 November 2020, 112666,https://doi.org/10.1016/j.ejmech.2020.112666

Iglesias, A. L., Miranda-Soto, V., Pompa-Monroy, D. A., Martinez-Ortiz, J. G., Diaz-Trujillo, G. C., & Villarreal-Gomez, L. J.,2019, vol. 81, no. 2.https://doi.org/10.36468/pharmaceutical-sciences.515

Hassan, S. Y.,Molecules, 2013, vol. 18, no. 3, Art. no. 3.https://doi.org/10.3390/molecules18032683

Shilpy Aggarwal, Deepika Paliwal, Dhirender Kaushik, Girish K. Gupta and Ajay Kumar, Combinatorial Chemistry & High Throughput Screening, Volume 21, Issue 3, Mar 2018, p. 194 - 203, https://doi.org/10.2174/1386207321666180213092911

Naglah, A. M., et al.,Pharmaceuticals, 2024, vol. 17, no. 5, Art. no. 5.https://doi.org/10.3390/ph17050655

Bekhit, A. A., & Abdel-Aziem, T., 2004, vol. 12, no. 8, pp. 1935–1945.https://doi.org/10.1016/j.bmc.2004.01.037

Nitulescu, G. M., et al., 2023, vol. 28, no. 14, Art. no. 14.https://doi.org/10.3390/molecules28145359

Matta, R., Pochampally, J., Dhoddi, B. N., Bhookya, S., Bitla, S., & Akkiraju, A. G., BMC Chemistry, 2023, vol. 17, no. 1, p. 61.https://doi.org/10.1186/s13065-023-00965-8

Mohammad A Alam, Future Medicinal Chemistry, 2022, Vol 14, No 5, pages 343-362 https://doi.org/10.4155/fmc-2021-0275

Ceramella, J., Iacopetta, D., Catalano, A., Cirillo, F., Lappano, R., & Sinicropi, M. S., 2022, vol. 11, no. 2, p. 191.https://doi.org/10.3390/antibiotics11020191.

Sangshetti, J. N., JMPAS, 2022, vol. 11, no. 4, pp. 5108–5121.https://doi.org/10.55522/jmpas.V11I4.3068

Mandal, S., et al., 2025, vol. 1323, p. 140738.https://doi.org/10.1016/j.molstru.2024.140738

Moussa, Ziad et al., Heliyon, Volume 10, Issue 20,https://doi.org/10.1016/j.heliyon.2024.e38894

Katariya, D., and M. Borisagar, *Russian Journal of Organic Chemistry* 60, no. 12 (2024): 2475-2482, https://doi.org/10.1134/S1070428024120224

****